

# A novel method for the evaluation of particle sharpness

by N.R. Steward\* and H. Ruthert†

## SYNOPSIS

An understanding of wear in systems conveying solids is extremely important from the standpoints of design and economics. The lifetime of any bulk solids-handling system depends on the type of solids present and the operating parameters of the transportation system. The relationship between wear in backfill pipelines on South African gold mines and the transportation system's operating parameters is well understood. However, the effect of the transported solids on the pipe wear is less well understood, because of an inability to characterize particle sharpness. The sharpness of the particles, together with their size and hardness, is responsible for the aggressivity of particles, or their ability to cause damage and wear.

This paper presents a novel method for the characterization of particle sharpness. The results presented rank particles according to the sharpness of their surfaces.

## SAMEVATTING

'n Begrip van die slytasie in stelsels wat vaste stowwe vervoer, is uiters belangrik uit die oogpunt van ontwerp en ekonomie. Die lewensduur van enige stelsel vir die massahantering van vaste stowwe hang van die soort vaste stowwe aanwesig en die bedryfsparameters van die vervoerstelsel af. Die verhouding tussen die slytasie van terugvulpleidings in Suid-Afrikaanse goudmyne en die bedryfsparameters van die vervoerstelsel word goed begryp. Die uitwerking van die vaste stowwe wat vervoer word op die pyplytasie word egter nie so goed begryp nie, vanweë 'n onvermoë om die skerpte van die partikels te karakteriseer. Die skerpte van die partikels, tesame met hul grootte en hardheid, is verantwoordelik vir die aggressiwiteit van partikels, of hul vermoë om skade en slytasie te veroorsaak.

Hierdie referaat bied 'n nuwe metode om die skerpte van partikels te karakteriseer. Die resultate wat aangebied word, rangskik partikels volgens die skerpte van hul oppervlakke.

## INTRODUCTION

Although the phenomenon of particle sharpness is well documented<sup>1–8</sup>, its effect on the system within which it occurs has yet to be quantified. Steward<sup>1</sup> has shown that the degradation of particles can lead to dramatic decreases in the wear rate of pipeline materials under conditions of hydraulic transport. Particle degradation can be defined as a decrease in both particle size and sharpness. Various authors<sup>1–3,6,9–11</sup> have observed that particles become rounded during their hydraulic transportation through pipelines. This particle degradation is attributed to 'autogenous milling' within the pump and the pipeline. Methods of quantifying the decrease in particle size and the rounding process have been suggested<sup>6,9–11</sup>, but both the quantification and the contribution made by these two particle parameters to the wear process remain elusive.

This paper addresses the problem of particle sharpness and presents a novel method for its evaluation. It is essential that the reader should understand exactly what is sought. In general, the concepts of particle shape and sharpness are often confused or taken to be the same. The effect of particle sharpness has been discussed by many authors<sup>2,5,7,8,12–18</sup>, but they give no real definition of particle sharpness other than common statements like 'the sharp grain slurry contained sharp sand' (Wang<sup>7</sup>) and 'angular particles will cause more wear than rounded ones' (Truscott<sup>2</sup>).

This vagueness is due to the lack of an effective method of determining the abrasivity of a particle. A definition of particle sharpness is required over and above the shape

description given by *British Standard 2955* of 1958, which is as follows:

Acicular	Needle-shaped
Angular	Sharp-edged or having a roughly polyhedral shape.

Even the standard applies to particle shape; in fact, it correlates shape and sharpness, i.e. 'angular' being equated to sharp-edged.

Based on the research presented in this paper, the following description of particle sharpness is proposed: particle sharpness is the degree to which the perimeter of a particle changes over its total length, and the rate of each change on that perimeter.

A direct evaluation of particle surface requires measurements of the surface. The evaluation of particle angularity proposed here is based on measurements of an image of the particle. The image can be obtained by conventional photography, by digital imaging, or by any other method that produces an image of the particle under evaluation. Depending on particle size, the image can be captured through either a microscope or a macro-lens. The use of a two-dimensional image necessarily reduces the three-dimensional particle surface to a projected image of the particle from which all the particle's surface parameters, size, shape, and angularity are determined.

The projection of a particle onto a surface is related to a true section through the particle only in exceptional cases. There is no unique way in which a particle comes to rest when placed on a surface, the number of possible particle orientations varying from six for a cube to infinity for a sphere. At first this may appear to be an argument against the use of a particle's projection as a representative indicator of particle surface characteristics. However, it can be argued that

\* 6 Selbourne Road, Sea Point 8001.

† University of Cape Town, Private Bag, Rondebosch 7700.

© The South African Institute of Mining and Metallurgy, 1993. SA ISSN 0038-223X/3.00 + 0.00. Paper received November 1992; revised paper received March 1993.

- (1) the larger the number of possible projections of a specific particle, the more random is the choice of a section, and therefore the more statistically representative the sample;
- (2) the more a particle deviates from a sphere, the lower is the number of possible projections but, at the same time, the chance increases of the particle displaying the projection most representative of those surface characteristics relevant to the wear process.

The second argument is best supported by the example of a needle, as demonstrated in Figure 1. In terms of wear, the point of a needle gouging into a surface is going to cause more damage to the surface than a needle sliding along the surface on its side. It is not intended to use the particle projection in isolation; instead, it must be seen as a contribution to the overall analysis of the wear characteristics of a particle.

### PARTICLE ANGULARITY

The angularity of a particle, called the angularity index, is calculated from a relationship between particle sharpness and size and the Particle Perimeter Angularity Measurement Relationship (PPAMR), which generates a direct measure of the average angularity of the particle's protuberances. This method is explained with the help of Figures 2 and 3.

Figure 2 is the diagrammatic representation of the projected image of a particle with four sides (AB, BC, CD, DA) and four angles ( $\alpha_1$ ,  $\alpha_2$ ,  $\alpha_3$ ,  $\alpha_4$ ). The external angles of the protuberances are measured and summed, and the average is calculated through division by the number of protuberances measured. The resulting number is referred to as the angularity index (AI) for that specific particle.

$$AI = \frac{\sum_{i=1}^n \alpha_i}{n} \quad \text{for } \alpha_i > 180^\circ,$$

where

- $\alpha$  = the external angle of protuberances in the particle
- $n$  = the number of angles measured.

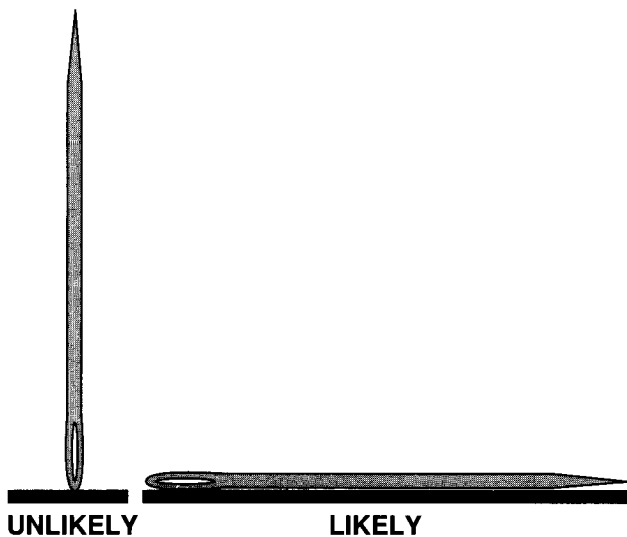


Figure 1—Orientation of a needle at rest

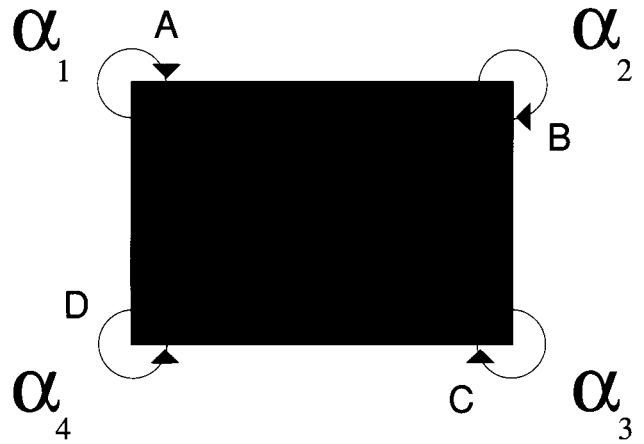


Figure 2—Simple representation of a particle

Figure 3 shows a more complicated particle projection, and serves to explain in greater depth the concept behind this method of measurement. Changes in the outline of the particle projections that extend into the body of the particle result in surface characteristics with angles that are less than 180 degrees ( $\alpha_3$ ). These surface characteristics give rise to no damage to the pipeline material on impact, and are therefore not included in the calculation of the AI. Only protuberances with angles greater than 180 degrees are measured for inclusion in the index. Angles 1 to 14 (excluding angle 3) of the particle are measured and treated as described in Figure 2, resulting in the required index. The particle outline forming the curved section of the projection is effectively reduced to a polygon by this method of measurement, the length of each side being determined by the resolution of the measuring technique.

While the PPAMR can be calculated manually with a ruler, it is tedious and will result in the evaluation of only a few particles. If a dimensionless list of the data points forming the perimeter of the particle image is transferred to a computer, the measurement process can be carried out quickly and accurately. With the advances in computer-based image-processing systems, not only can the measurement procedure be automated, but it can capture the initial data from an actual particle.

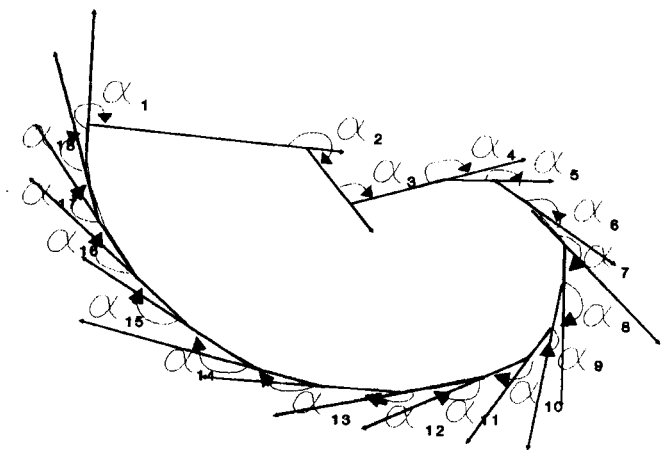


Figure 3—Representation of a particle image

## PARTICLE IMAGE ANALYSIS

Data on particle characteristics that are to be used for calculation purposes have two essential requirements:

- (a) the parameters affecting the problem under research must be clearly defined,
- (b) the measurement of these parameters must yield reproducible quantitative results.

The solids transported in industrial or mining applications generally have a wide size distribution, and not a single or limited size range. The means that particles of varying sizes must be evaluated, and the following automated system is suggested to analyse the large numbers of particles that constitute a representative sample.

### The System

The automation of particle measurement, besides utilizing a complex program, requires the computer to 'see' the particles under analysis and then analyse what it has 'seen' to extract the necessary information. This translates into a system that involves both remote sensing and image analysis.

Remote sensing constitutes the 'seeing' aspect of the system. When a computer manipulates data from any 'visible' region, be it magnetic, infrared, X-ray, or visible, it is called image processing. The system used in this research was developed in the Department of Surveying at the University of Cape Town by H. Ruther. The system, called PHOENICS (PHOtogrammetric ENgineering and Industrial digital Camera System), is a computer-based near-real-time-photogrammetry (NRTP) system. Ruther and Parkyn<sup>19</sup> describe PHOENICS in detail. The layout and equipment used in the system for this research, with the exception of the microscope, are essentially the same as for the PHOENICS system (Figure 4).

### The Computer

A personal computer was used on the basis of past experience with computer-based NRTP. The system is equipped with a microprocessor running at 25 MHz, a 32-bit internal bus, an 80387 mathematics co-processor, and a super VGA 14-inch colour screen. This screen is used as the command screen, the images being displayed on an external monitor (type TVM MD-11), which is a multi-

function colour monitor with resolutions from 640 by 200 up to 1024 by 768 and a 0,31 dot pitch. The application in conjunction with the image-processing card requires it to be used as an analogue monitor displaying a monochrome image.

### The Camera

The camera chosen for this system is the Panasonic WV-CD 20. It is a monochrome solid-state TV camera with a CCD chip or image sensor. The CCD chip or sensor is of the interline transfer type, and has the dimensions 8,8 by 6,6 mm, which is equivalent to the scanning area of a 2/3-inch vidicon tube. The resolution of the sensor is 500 horizontal pixels by 582 vertical pixels, which gives a pixel size of 17 by 11  $\mu\text{m}$ . The scanning system is a 2:1 interlace with 625 lines at 50 Hz, which provides a frame rate of 25 Hz. The output of the camera is in the form of a continuous analogue amplitude modulated signal. This requires conversion to the digital form for the computer to carry out any analysis. The conversion is performed by an analogue/digital (A/D) converter.

### Video Frame Grabber

The frame grabber, in this case a MATROX PIP-512 board, is dedicated to the A/D conversion, frame grabbing, and storing of the frame. The frame is the image under analysis. The A/D converter converts the analogue signal from the CCD camera into 8-bit pixels, which results in shades of grey ranging from 0 for black to 255 for white. The process of capturing the image for the subsequent manipulation or viewing has been described by Ruther and Parkyn<sup>19</sup>. They detail the following six steps in the operation.

- (1) Image integration and transfer on the CCD sensor. (In the case of this research, the image was captured through a microscope.)
- (2) Output of the image in analogue form.
- (3) Digitizing of the video image, i.e. conversion of the analogue signal into 8-bit bytes by means of an A/D converter.
- (4) Passing of the data through a LUT (look-up table), in which the grey values coming from the camera are transformed for output in a user-selected form (for example, transformed from positive to negative image, contrast enhanced, or thresholded).

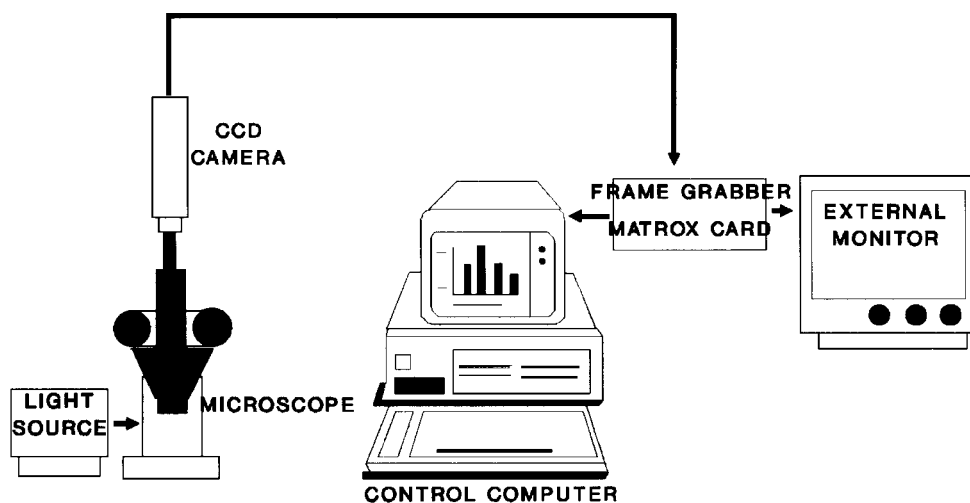


Figure 4—The image-processing system

- (5) Storing of the image in the board buffer
- (6) Conversion of the image from digital to analogue (D/A converter) for display on a monitor. (This step is not essential since the image does not necessarily need to be displayed.)

The MATROX PIP-512 image-processing board converts the analogue signal of the image coming from the CCD camera into a 512 by 512 8-bit pixel array. This image can be held in the video buffer of the board or can be transferred to the system's storage facility, hard disk, floppy disk (5-inch), or stiffy disk (3-inch). The MATROX board has a number of built-in image-processing techniques to manipulate the images captured. The board's operations can be controlled through external programs, which, as is the case with the program written for this research, instruct the board to perform specific operations on the captured image stored in the board's buffer. The MATROX board can support computer languages such as FORTRAN and C. The programs used in the research described here were written in C.

### **The Microscope**

Because of the particle-size distribution within a slurry, ranging from some 20 mm to dust, the finer particles have to be magnified in order to be resolved. The CCD camera is attached to the microscope so that images from magnifications of 5X to 64X can be captured by the MATROX board. The Nikon SMZ-2T stereo-microscope allows for various lighting methods to be tried. The only drawback in the use of a microscope for this research was the poor field of vision for this work, in which thousands of particles had to be evaluated. It is recommended that a macro-lens should be used wherever possible.

### **Principles of Automatic Image Capture**

Information about the image is gathered according to the signal modulation, the grey level, in an image. Therefore, the grey levels associated with the information to be collected must be clearly separated from any extraneous or insignificant information. This is achieved through the sample preparation and thresholding.

The sample to be analysed is prepared in such a manner that it has the greatest possible contrast to its background, i.e. black on white. This optical information is then converted, picture point by picture point, into an electrical signal that is initially stored in the buffer of the frame grabber. Thresholding of an image further discriminates between the captured image and any noise and extraneous information present in the captured frame. Once the image has been thresholded, resulting in a binary image of either information or background, a working image is captured and transferred to the buffer of the image-processing card (IPC). Information on the image characteristics can be determined from the image, or images, in the captured frame according to the program manipulation of the stored thresholded data on the images.

### **IMAGE-PROCESSING PROCEDURE AND PROGRAM**

The generation of information or factors pertaining to the surface characteristics of a particle through image-processing techniques is discussed in this section.

## **Image Capture**

### **Thresholding**

The sample prepared for image analysis is viewed through a microscope or macro-lens, which is connected to the CCD camera, and through the image-processing card, which is displayed on the high-resolution analogue screen. A grey-level histogram is constructed of the digitized image, and is displayed on the command screen. This histogram represents the number of occurrences of a particular pixel intensity value throughout the displayed image. The intensity level corresponds to a grey-scale level with values between 0 and 255. The IPC software carries a facility for the generation of such a histogram. If the contrast between the image and the background were perfect, the histogram would represent the total image on the analogue screen as a binary image of only black (0) and white (255) grey levels. In reality, however, there are many other shades of grey, with values between 0 and 255, that make up any image. The histogram, once displayed on the command screen, gives an indication of the background grey level in relation to the particle's grey level. A threshold value is now chosen that differentiates between those grey levels constituting the background and those of the sample. Thresholding the image results in the displayed image on the analogue screen being converted to the desired binary image. This process is carried out in conjunction with the display of the intensity histogram on the command screen. The binary image is achieved through the IPC software, involving LUT and scaling operations. These functions have the combined effect of changing the scale of the established LUT, which is the table used for mapping the original 512 by 512 image. These two functions are controlled by the threshold value returned from the command screen histogram. The threshold value to be selected can be varied by the movement of a cursor along the histogram parallel to the Y-axis along the X-axis. The X-axis represents the grey levels present in the original image. The movement of the cursor changes the scaling and LUT and, thus, the binary image displayed on the analogue screen. When the best possible binary image corresponding to the true image is obtained, the threshold value associated with the currently displayed binary is selected from the histogram. The scaling function maps the original grey levels onto new grey levels, using the thresholding value as an index to the LUT, and the new grey level (0 or 255) as the new mapped value (Figure 5). In the case of this research, only one scaling function is necessary since only a binary image is required. Therefore, the LUT is broken into only two parts: black and white, 0 and 255. When the required binary image is displayed on the analogue screen, it is 'snapped' or captured, transferring it to the IPC frame buffer.

### **Storage of Images**

The binary image stored in the buffer of the MATROX card is transferred to the chosen mass-storage medium. The transfer is carried out under a given file designation through the command screen. The routine involving image capture and storage can be carried out on a number of images prior to analysis.

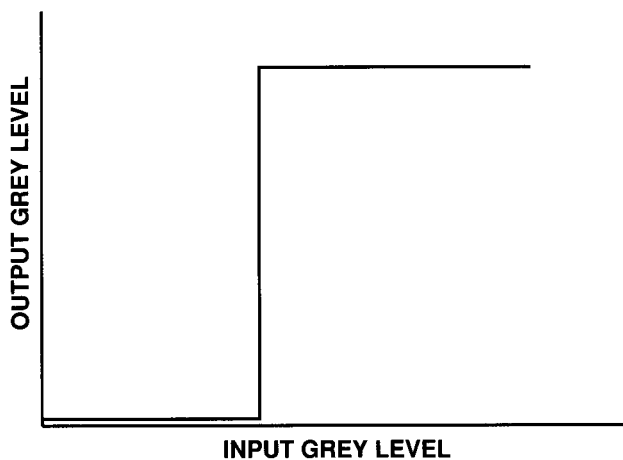


Figure 5—Thresholded lookup table

### Edge Detection

On retrieving an image from the mass-storage medium in its threshold format, an edge-detection routine is automatically carried out on the particle images. This technique finds and returns only those pixels falling on the perimeter of the particle image. The pixels forming the internal area of the particle image are discarded. This method of edge detection involves a comparison of sequential pixels from left to right. Each pixel has a numerical value relating to its grey level, either 0 or 255. The method used to detect the edge of a particle is a simplification of a standard-gradient or differential method. Simplification is possible because of the assumption of only two values in any image, either 0 or 255.

The method is explained with reference to a horizontal traverse across Figure 6. In comparing two pixels, consider pixel (1,2) and (1,3), with values  $x$  and  $y$ . The values  $x$  and  $y$  are the values of the original image irrespective of any changes made by the following calculations. A value  $z$  is determined where  $z = (y - x)$ . If  $y$  is greater than  $x$  ( $y > x$ ), then  $z$  is greater than 0 ( $z > 0$ ), and a positive edge is determined, i.e. the particle edge starts at pixel (1,3). Pixel (1,3) is thus set to a value of 255. Consider pixels (2,6) and (2,7),  $x$  and  $y$  respectively. If  $x$  is greater than  $y$  ( $x > y$ ), then  $z$  is less than 0 ( $z < 0$ ) and a negative edge is detected, i.e. the particle ends at pixel (2,6). Pixel (2,6) is thus set to a value of 255. If  $x$  is equal to  $y$  ( $x = y$ ), i.e. pixels (2,3) and (2,4), then there is no edge, and pixel (2,4) is set to 0 irrespective of the original value. This process is repeated twice, once in the horizontal axis and once in the vertical axis.

The reason for this can be seen by reference to Figure 6. In a horizontal traverse, the edge at pixel (1,4) would be lost since pixel (1,3) would be picked up as the positive edge and pixel (1,5) as the negative edge; pixel (1,4) in comparison with (1,3) would return a  $z$  value of 0, indicating no edge. By means of a vertical traverse, lost edges such as that described above would be found. The two sets of values are averaged,  $c = (x + y)/2$ , to prevent overflow of the pixel value, i.e. to maintain the maximum grey-scale value at 255. It is important to note that this process does not log the data points forming the perimeter of an individual image. It is a method of simplifying the image's outline for the subsequent line following according to the routine required to log the perimeter data points. The

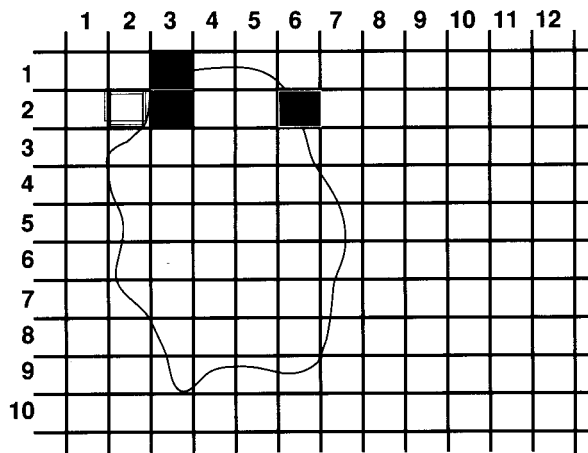


Figure 6—Edge-detection method

perimeter point-logging routine is carried out as a subroutine in the image-edit and particle-analysis routines.

The line-following routine is discussed here with reference to Figure 7. Pixel (2,7) is the first found as having a pixel value of 255. A search around this pixel is then initiated, beginning at pixel (1,7) to pixel (1,6) to pixel (3,6), where the following pixel is found. Each pixel around (3,6) is then searched in a clockwise manner, starting with (2,6). The next pixel found is (3,5). After each pixel with a value of 255 is found, it is set to zero, effectively 'destroying' the image's perimeter. The entire perimeter is searched in this manner until pixel (2,7) is returned to. The points on the image's perimeter are now stored for use in the analysis of various particle characteristics.

### MEASUREMENT OF PARTICLE ANGULARITY

With reference to Figure 8, the technique of automated measurement is carried out in the following manner. Starting at point (1,1), a vector (a) 3 pixels long is drawn through the following 3 pixels forming the image outline. The reason for the vector being longer than 2 pixels depends on the nature of the image representation, i.e. through pixels. Pixels are essentially square in shape, and this leads to an image's perimeter being effectively constructed from steps. Therefore, if every change in the

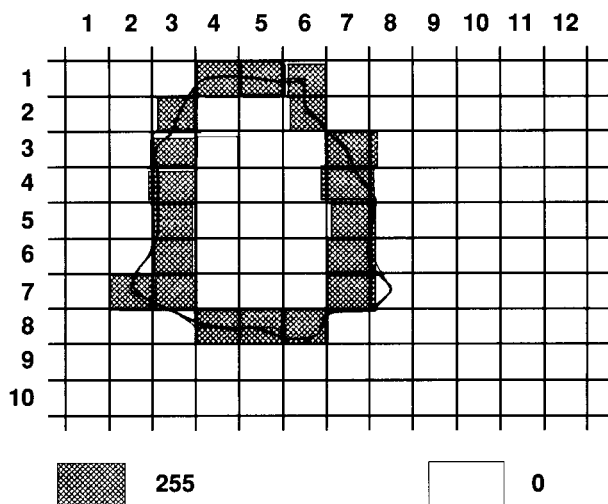


Figure 7—Line-following method



processing system and the system configuration described in this paper generate an index for particle sharpness that reflects the texture of the image perimeters of a particle. Whether or not image processing is effective as an indicator of a particle's aggressivity (or its ability to cause damage and wear), will require an analysis of pipeline-transported particles and the resultant pipe wear.

## REFERENCES

1. STEWARD, N.R. The wear of materials in hydraulic transport pipelines. M.Sc. thesis, University of Cape Town, 1988.
2. TRUSCOTT, G.F. A literature survey on wear in pipelines. Cranfield (UK), BHRA Fluid engineering, TN 1295, 1975.
3. BAKER, P.J., and JACOBS, B.E.A. *A guide to slurry pipeline systems*. Cranfield (UK), BHRA Fluid Engineering, 1979.
4. JACOBS, B.E.A., and JAMES, J.G. The wear rates of some abrasion resistant materials. 9th International Conference on the Hydraulic Transport of Solids in Pipes, Rome, 1984. Paper G3.
5. SAUERMANN, H.B. Pump and pipe wear. *HYDROTRANSPORT 9*. Johannesburg, 1982. Chap.12.
6. SHOOK, C.A., HASS, D.B., HUSBAND, W.H.M., and SMALL, M. 6th International Conference on the Hydraulic Transport of Solids in Pipes, Rome, 1979. Paper C1.
7. WANG, Q. Wear resistance of steels under wet-abrasive erosion conditions. *Wear*, vol. 112. 1986. pp. 207-216.
8. MARCUS, R.D. Wear on freight pipelines—a limiting factor? *S. Afr. Mech. Engr*, vol. 34. Mar. 1984. pp. 80-86.
9. KARABELAS, A.J. Particle attrition in shear flow of concentrated slurries. *AIChE*, vol. 22, no. 4. 1976. pp. 756-771.
10. LAMMERS, G.C., ALLEN, R.R., DONOVAN, D.J., WAGNER, E.O., and PERRY, V.F. US Bureau of Mines, *Report 5404*.
11. DEVASWITHIN, A., and PITCHUMANI, B. An approach to study the particle degradation during impact. *Bulk Solids Handling*, vol. 7, no. 4. 1987. pp. 547-550.
12. LINK, J.M., and TUASON, C.O. Pipe wear in the hydraulic transport of solids. *Mining Congress J.*, 1972, pp. 38-44.
13. OETTEL, R. Hydraulic mining and hydraulic transport. *Braunkohle Wärme und Energie*, vol. 13, 1961. pp. 341-354. (Translated for C.E.G.B., Transln No. 2571).
14. WORSTER, R.C., and DENNY, D.F. Hydraulic transport of solid material in pipes. *Proc. Instn Mech. Engrs*, vol. 169, no. 32. 1955. pp. 563-573.
15. ABU-ISA, I.A., and JAYNES, C.B. Mechanism of abrasion of elastomers by small particle impacts. International Rubber Conference, IRC 86, Goteborg, 1986.
16. EPHITHITE, H.J. Rubber lining—the soft option against abrasion. *Bulk Solids Handling*, vol. 5, no. 5. Oct. 1985. pp. 1041-1047.
17. GOODWIN, P.J., and RAMOS, C.M. Degradation of sized coal at transfer points. *Ibid.*, vol. 7, no. 4. Aug. 1987. pp. 517-534.
18. STEWARD, N.R., and HECKROODT, R.O. Resistance of polymeric materials to slurry abrasion. 7th International Conference on Erosion by Liquid and Solid Impact, Cambridge, 1987.
19. RUTHER, H., and PARKYN, N. The development of a PC-based near-real-time photogrammetry system. International Congress ISPRS, Kyoto, 1988.
20. STEWARD, N.R., and SPEARING, A.J.S. The effect of particle sharpness on the wear of backfill pipelines. *J. S. Afr. Inst. Min. Metall.*, vol. 93, no. 5. May 1993. pp. 129-134 (this issue).

## BOOK Review

### **Mining and metallurgy in Australia**

Reviewer: H.G. Mosenthal

*Down Under: Mineral heritage in Australasia. An illustrated history of mining and metallurgy in Australia, New Zealand, Fiji and Papua, New Guinea*, by Arvi Parvo. Melbourne, The Australasian Institute of Mining and Metallurgy, Monograph 18, 1992. Hardback 280 mm x 210 mm, 310 pp. \$A40 (members), \$A50 (non-members).

Sir Arvi Parvo is Chairman of Broken Hill Proprietary Company, Limited, Western Mining Corporation, and Alcoa. He studied mining at Clausthal Mining Academy and at the University of Adelaide, where he graduated with First Class Honours in 1956.

During his year of office in 1990 as President of the Australasian Institute of Mining and Metallurgy (AusIMM), he visited and addressed the many branches that make up the AusIMM. The addresses gave a historic review of mining and metallurgical operations in the areas served by the various branches. These talks have now been assembled into book form, and make for a most interesting and readable account of mining Down Under.

Australian mining started in Newcastle in 1800. At that time, coal was exported to India and the Cape of Good Hope. Gold discoveries in Victoria at Bendigo and Ballarat followed in 1851. The Broken Hill lead-zinc deposit was discovered in 1883. The Western Australian gold mines,

like their Witwatersrand counterparts, were opened in 1886. Kalgoorlie and Coolgardie, the most famous, were developed in 1893. Mount Isa Mine in Queensland dates back to 1923—a relatively new mine. The uranium deposits at Mary Kathleen and Rum Jungle were discovered during the Second World War.

More recent developments concern bauxite in the Gulf of Carpentaria, iron ore in the Pilbara region of Western Australia, and Bougainville Copper and OK Tedi in Papua New Guinea.

Each Australian State is given a section of the book. A section consists of as many as six chapters—a chapter being a paper that was presented to a branch. Three additional sections cover mining in New Zealand, Fiji, and Papua New Guinea.

The AusIMM was founded in 1893 in Adelaide, South Australia. It is therefore a year older than our own Institute. In 1990, its 38 branches had a total of 7840 members (considerably larger than the SAIMM), and its strength is due to the very active branches countrywide.

Sir Arvi Parvo has produced an entertaining history. To someone whose knowledge of Australasian mining is limited, the many maps, illustrations, and historic pictures in the volume bring it to life.

